scientific reports

Check for updates

OPEN

Functional characterization of a type I-F1 CRISPR-cas system from the clinical isolate *Shewanella xiamenensis* Sh95 reveals constitutive activity and plasmid-curing capability

María Carolina Molina[1,2] & Cecilia Quiroga[1,2]✉

CRISPR-Cas are prokaryotic adaptive immunity defense systems that provide protection through RNA-guided recruited nucleases effectors.Despite the vast diversity in which CRISPR-Cas systems naturally exist, the single effectors from Class 2 were the most studied as genetic engineering tools. Later, the endogenous reprogramming of type I CRISPR-Cas systems showed promising results in diverse bacteria. However, the features and functions of the subtype I-F1 from *Shewanella* spp. members remain poorly characterized. Here, we report the analysis of the genetic context and activity of a type I-F1 CRISPR-Cas system within the species from the clinical isolate *Shewanella xiamenensis* Sh95 (SxCRISPR-Cas3). We show that this system transcribes constitutively and contains an internal promoter within *cas3f* open reading frame. Using endogenous reprogramming assays with synthetic mini CRISPR arrays, we demonstrate that the system is functionally active producing target plasmid interference and plasmid curing. Together, these results represent a simple methodology for obtaining colonies of *S. xiamenensis* Sh95 cured from the target plasmid and lay the foundation to the future exploration of SxCRISPR-Cas3 as a programmable interference tool.

Shewanella spp. are gram-negative, facultative anaerobic, motile, and rod-shaped bacteria, that are considered important as microbial fuel cells and bioremediators of polluted environments[1–4]. The identification of multidrug resistant (MDR) isolates as well as the increase in opportunistic human infections reports worldwide led to the categorization of the genus as a group of emerging pathogens[5–8]. *Shewanella* spp. holds intrinsically a high accessory genome plasticity, and it was previously implicated not only as an environmental reservoir of *qnrA*, *oxa-55*, and *oxa-48-like* variants, but also as the vehicle for the dissemination of these antimicrobial resistance genes (ARGs)[5,9]. For these reasons, the genetic manipulation of members of this genus is highly desirable[10]. Classical bacterial genome engineering techniques tend to be limited to a handful of extensively studied species and while genetic modification of refractory non-model bacteria has proven difficult, the use of different types and formats of CRISPR-Cas systems increased the recovery of *Shewanella* spp. recombinants[10–13].

CRISPR-Cas are prokaryotic adaptive immune systems whose defense functions depend on RNA-guided nucleases that recognize specific sequences of invading phages and plasmids[14–17]. A wide variety of systems exist in nature, classified into 2 classes and 44 variants[18]. The most abundant and diverse group is class 1, whose systems depend on multiprotein effector complexes, and among which, the majority correspond to type I[18,19]. Despite this fact, members of class 2 became the most studied and applied systems[20,21]. Endogenous reprogramming of different type I CRISPR-Cas systems, including subtypes I-A, -B, -C, -E, -F, and -G, has been demonstrated in several bacteria by providing synthetic CRISPR RNA guides *in trans* into strains harboring functional native systems[22]. In particular, subtype I-F1 CRISPR-Cas systems have been repurposed for diverse applications across multiple bacterial hosts[21,23–27]. Previous analyses showed that 4 different types of CRISPR-Cas systems (I-E, I-F, III-B, and VI-A) are encoded in *Shewanella* spp. genomes and that the type I-F is the most frequent[5]. In *S. xiamenensis* strains, subtypes I-E, III-B, and I-F were reported[5,28].

[1]Universidad de Buenos Aires, Facultad de Medicina, CABA, Argentina. [2]CONICET, UBA, Instituto de Investigaciones en Microbiología y Parasitología Médica (IMPaM), CABA, Argentina. ✉email: cquiroga@fmed.uba.ar

Despite type I CRISPR-Cas systems being prevalent in *Shewanella* spp[5,29]. , several studies have focused on the heterologous deployment of established CRISPR-Cas based tools into the model strain, *S. oneidensis* MR-1, achieving gene regulation and editing[11,30–35]. Comparative assays of different systems in the model strain, *S. oneidensis* MR-1, showed that a heterologous Cascade complex from the type I-F1 of *Pseudomonas aeruginosa* (PaeCascade) achieved higher repression efficiency than the genus-native I-F2 variant and a heterologous type I-G[11], underlining functional differences between related subtypes in *S. oneidensis* MR-1, which lacks a native CRISPR-Cas system[5].Within the *Shewanella* genus, biochemical and functional characterizations were performed in the "minimal" variant of type I-F (currently classified as subtype I-F2) from *Shewanella putrefaciens* CN-32[36,37]; the target interactions of the type I-F1 from *S. baltica* OS195 were also evaluated[32]; and more recently, the heterologous and endogenous integration activity of the type I-F3 CAST from *Shewanella* sp. ANA-3 was shown[38]. Accordingly, investigating native type I-F1 CRISPR-Cas systems from *Shewanella* spp. is important for understanding their unique molecular features expanding their potential for DNA targeting applications.

Here, we report the functional characterization of the type I-F1 CRISPR-Cas system from the clinical isolate, *Shewanella xiamenensis* Sh95 (SxCRISPR-Cas3). Comparative genomic analysis revealed the surrounding genetic context of this system, including several upstream and intergenic rearrangements and an insertion sequence of the IS*256* family (IS*Sod4*) located near *cas1*. Transposition events into CRISPR-Cas loci were proposed to act as transcriptional inhibition mechanisms that could produce transcriptional inactivation of these defense systems, thereby facilitating the acquisition and dissemination of mobile genetic elements (MGEs)[39]. In addition, IS*256* family elements were implicated in modulating the expression of antibiotic resistance genes through the generation of hybrid promoter sequences resulting from transposition events[40]. RT-PCR analysis showed that this system is constitutively transcribed, and promoter prediction combined with experimental validation identified an intragenic constitutive promoter within *cas3f*. Finally, we demonstrated that this system is functionally active through endogenous reprogramming directed against a target plasmid and present a simple methodology that enabled the recovery of *S. xiamenensis* Sh95 colonies cured of the target plasmid.

Results

SxCRISPR-Cas3 system genomic context

S. xiamenensis Sh95 has a type I-F1 CRISPR-Cas system composed of 6 *cas* genes *cas1-cas2/3(cas3f)-csy1(cas8f1)-csy2(cas5f1)-csy3(cas7f1)-csy4(cas6f)* with a single CRISPR array of 153 spacers immediately downstream of *cas6f* (Fig. 1A) access code LGYY00000000.1[41]. Repeat length corresponds to 28 nucleotides whilst spacer sizes vary between 31–33 bases. The spacer length of 32 bases was the most represented (> 95%) followed by 33 bp-long (3.92%) distributed across spacers #24, 40, 82, 110, 131, and 147, and the last spacer corresponds to 31 bp-long (0.65%). Two duplicated spacers were found in positions #88–89 and #148–149, respectively. Between the *cas* genes and the CRISPR array, a 155 bp-long AT rich sequence (77,4%) is located adjacent to the first repeat, consistent with the leader region (Fig. 1A). In this region, in the same orientation of *cas* genes coding strand, predictions pointed to a single putative promoter, and by further inspection, a potential IHF (Integration Host Factor) binding site sequence was identified (5'-ATACAATAAGTTA-3') located between positions + 60 to + 72 (taking the first nucleotide after *csy4* as + 1). This binding site is indispensable for spacer acquisition and shows conservation relative to the consensus sequence (5′-WATCAANNNNTTR-3′), matching location and coordinates previously reported in the leader region of other CRISPR-Cas systems[42]. The upstream region of SxCRISPR-Cas3 system sequence was determined by PCR, subsequent sequencing, and assembly of *S. xiamenensis* Sh95 contigs 66 (accession number NZ_LGYY01000278.1) and 16 (accession number NZ_LGYY01000138.1), where the former contained Sh95-*alpA-1* and a second *alpA* gene of putative phage origin named Sh95-*alpA-2* (for simplicity), whereas the contig 16 harbored the complete SxCRISPR-Cas3 system. The assembled sequence obtained by PCR was deposited in GenBank (accession number PX512296) and is listed in Supplementary File 2.

Genome comparison analysis revealed high nucleotide conservation of *cas* genes across diverse *Shewanella* spp. and *Vibrio* spp. strains (Fig. 1B and C). Interestingly, a loss in conservation is observed in several genomes for *cas3f*, *cas8f*, *cas5f*, and *cas7f*, whilst mainly *cas1* and in some cases also *cas6f* are the genes that retain overall conservation. Previously, this high level of diversity in the effector complexes was observed by comparison of I-F and I-Fv subtypes and the selective pressures from anti-CRISPRs were indicated as the plausible explanation[43]. Analysis of CRISPR repeats and spacers showed that the representative related I-F CRISPR-Cas systems displayed a homogenous 28 bp length and a conserved repeat sequence (when more than a single array was present, the closest to I-F *cas* genes was considered), although spacers showed length variations of 29, and 31 to 34 bases long (Supplementary Table S5). Regarding spacers, a variation in spacer's size distribution was found, with *S. xiamenensis* Sh95 and *S. decolorationis* Ni 1–3 displaying the longest CRISPR arrays, containing 153 and 113 predicted CRISPRs, respectively, meanwhile *V. cholerae* strains showed shorter arrays, the longest being in *V. cholerae* FORC_076 with 76 spacers (Supplementary Fig. S1A). In terms of spacer diversity, all related systems from the dataset contained spacers targeting phages, plasmids, and genomic island sequences (Supplementary Fig. S1B). Furthermore, in our dataset of related type I-F CRISPR-Cas systems the *cas* genes were found in proximity to putative genes coding for proteins containing HTH or WYL domains (Fig. 1B and C).

Comparison against the closest related type I-F CRISPR-Cas system from *Shewanella decolorationis* Ni1-3 showed insertion/deletion regions (Indels) upstream of Sh95-*cas1* consisting of the *alpA-2* spanning 615 bp (Indel 1) separated by 161 bp of homology from an insertion sequence (IS) of the IS*256* family where 1304 bp replace the sequence 5'-AAA-3' (Indel 2) present at position − 17 of *cas1* translational start site in *S. decolorationis* Ni1-3. Based on ISFinder analysis, this sequence likely corresponds to *ISSod4* with 99% identity, conserved inverted repeats (IR), and target site duplications (TSD) (Fig. 1D). The genome comparison analysis throughout the dataset showed that this IS*Sod4* is absent in other related I-F CRISPR-Cas systems, and although the gene Sh95-*alpA-2* was found in other genomes (*S. xiamenensis* DCB2-1, *S.*sp. POL2, partially in *S. xiamenensis* NUITM-

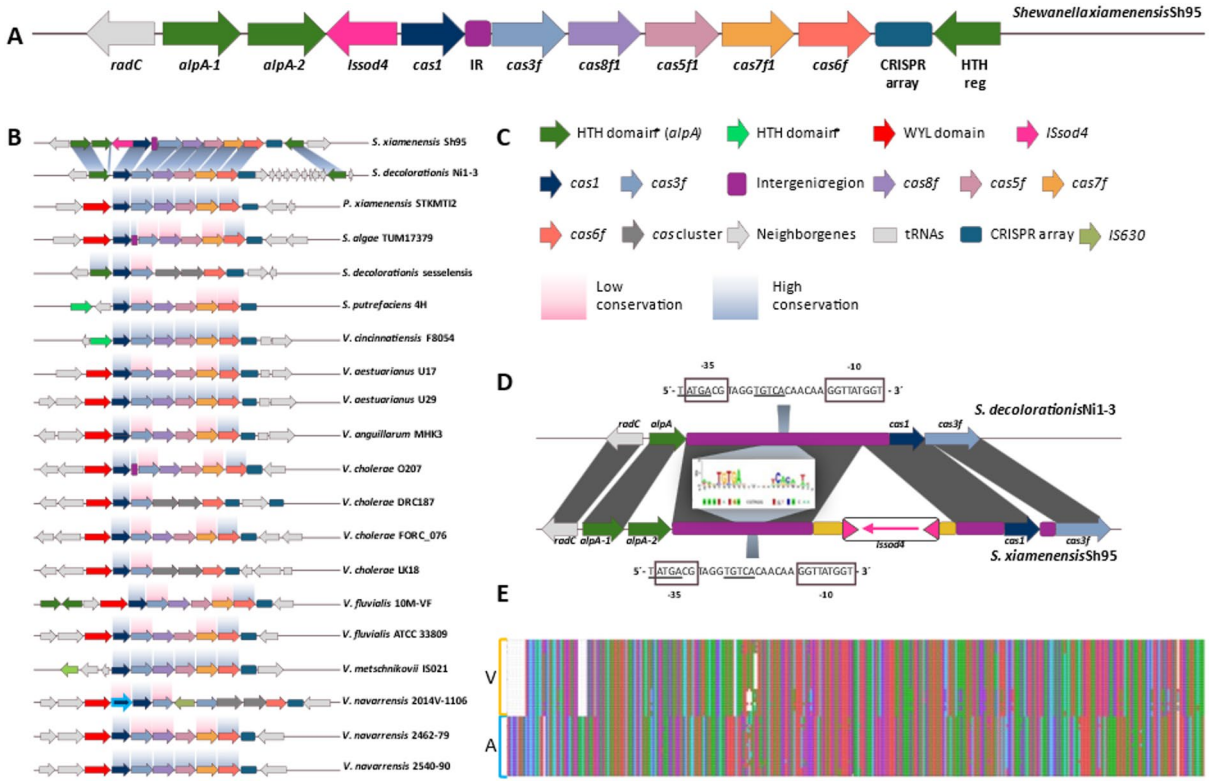

Fig. 1. I-F CRISPR-Cas systems related to SxCRISPR-Cas3 cluster with putative genes encoding HTH- and WYL- domains-containing proteins and some of them harbor an intergenic region of undetermined function. **A**) Schematic representation of the genomic context of SxCRISPR-Cas3 system. **B**) Comparison of 19 representatives of similar I-F CRISPR-Cas to SxCRISPR-Cas3 system shows the systematic presence of proximity putative genes coding for proteins with HTH or WYL domains. Genetics maps are not drawn to scale. **C**) Color and shapes code for schematics. HTH domain-containing protein coding genes* denote other HTH domain-containing putative proteins different from *alpA*. **D**) Detail of the comparison between *cas1* upstream regions of *S. xiamenensis* Sh95 and the most closely related I-F CRISPR-Cas system from *S. decolorationis* Ni1-3 showing the position of the possible original ancestor promoter. **E**) Multiple sequence alignments showing the conservation of the *cas1-cas3f* intergenic sequence among *Vibrionales* (V) and *Alteromonadales* (A).

VS1, and *Vibrio fluvialis* EKO3534197.1), it was not associated with an IS. Further analysis showed the presence of another Indel shaping an intergenic region of 382 bp between Sh95-*cas1* and Sh95-*cas3f* (Indel 3) (Figs. 1D and 2B). We performed a search of this sequence through the public database Integrated Microbial Genomes & Microbiomes system (IMG/M) (date: 10-18-24, see methods)[44,45]. Results yielded 8 matches that accounted only for *Shewanella* spp. genomes where all of them harbored a type I-F1 CRISPR-Cas system. Further examinations through GenBank database (10-18-24) in *Alteromonadales* and *Vibrionales* orders revealed only 22 *Shewanella* spp. strains genomes and 27 *Vibrionales* genomes that harbor this sequence, co-occurring in all cases with CRISPR-Cas systems (Fig. 2A). Interestingly, this intergenic sequence is highly conserved among the dataset (coverage range from 97 to 100%, and identity from 76,8 to 100%) (Fig. 1E) and despite maintaining the overall genetic architecture, similar I-F1 CRISPR-Cas systems harboring this intergenic locus show downstream loss of sequence identity (Fig. 2B).

Constitutive transcription and novel intragenic promoters detected in SxCRISPR-Cas3 system

Previous studies have shown that type I CRISPR-Cas systems transcriptional profiles vary from tightly regulated systems (I-E from *E. coli* K-12) to constitutively transcribed ones (I-F1 from *Pectobacterium*) and that different inducers participate in the induction of *cas* genes in response to a phage infection[46–52]. Bearing in mind that an endogenous reprogramming strategy for the SxCRISPR-Cas3 system will initially depend on the native expression profile of this system, we set out to verify its transcriptional activity. Considering that Sh95-*alpA-2* and IS*Sod4* together are not widely found in related I-F CRISPR-Cas systems of the dataset (Fig. 1B), we reasoned that these indels upstream of *cas1* in SxCRISPR-Cas3 could have disrupted the original regulatory locus of this system. Hence, we performed in-silico predictions to identify the possible promoter sequences, and a putative promoter with a conserved CRP box, consistent with Patterson et al. (2015)[53] results, was found in the intergenic region between Sh95-*alpA-2* and the IS*Sod4* (Fig. 1D). Notably, the conserved CRP box in *S. decolorationis* Ni1-3 was also present although between *alpA* and *cas1* (Fig. 1D). Although the transposition

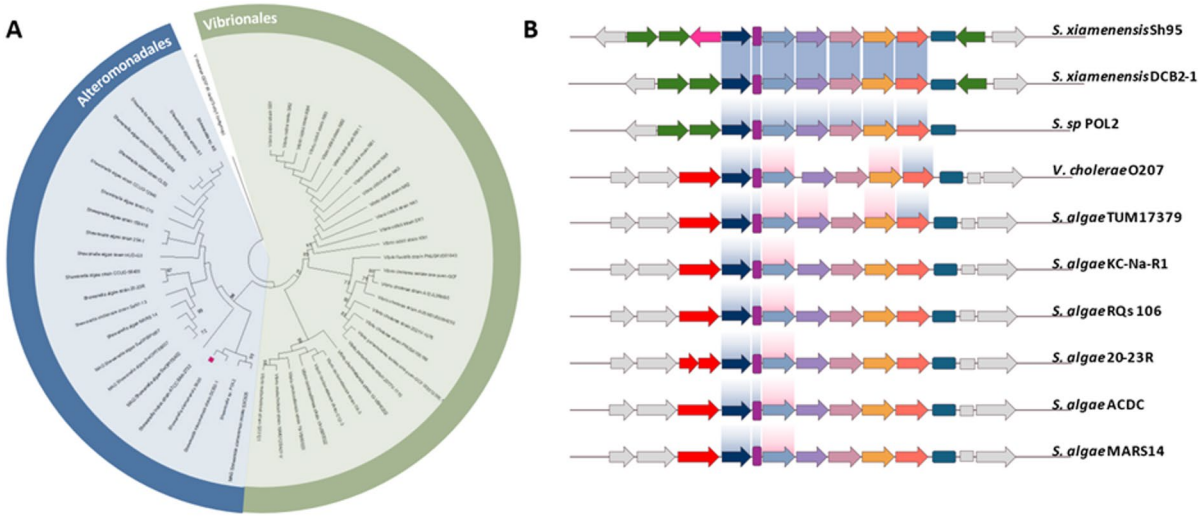

Fig. 2. Related to SxCRISPR-Cas3 systems retain the intergenic region and *cas1* conservation. **A**) Maximum likelihood tree built on the intergenic region *cas1-cas3f* found in *Alteromonadales* and *Vibrionales* taxa showing the distribution between the two distinct groups. *Shewanella* sequences span 382 bp long whilst *Vibrio* spp. intergenic regions length corresponds to 365 and 367 bp. Red square marks *S. xiamenensis* Sh95 in the tree. **B**) Comparative analysis of genetic architectures of systems related to SxCRISPR-Cas3 that also harbors the intergenic *cas1-cas3f* sequence. Colors and shapes follow the same code for the previous schematic diagrams.

event might have positioned this promoter far away from Sh95-*cas1* (at -1359 bp from the translation start site, TSS), our experimental analysis showed that the SxCRISPR-Cas3 system transcribes constitutively in the conditions assessed, most likely due to the presence of this promoter region (Fig. 3A, B and D). Genes *cas1*, *cas3f*, *cas8f1*, and *cas6f* were detected as a constitutively transcribed polycistronic transcript which was confirmed by producing first strand cDNA synthesis from a single specific reverse primer at *cas6f(csy4)* and subsequent PCR amplification (Fig. 3B and D). Transcriptional analysis of the CRISPR array by using a single reverse primer hybridizing spacer #147 for first strand cDNA synthesis confirmed that CRISPRs most likely transcribe in a polycistronic nature and in the same orientation of *cas* genes (Supplementary Fig. S2). We continued to explore whether the genomic arrangements influenced the SxCRISPR-Cas3 regulatory region by analyzing putative alternative promoter sequences. Correspondingly, we proceeded to clone a fragment spanning from positions 844 to 3486 of Sh95-*cas3f* which contained the putative promoters' sequences with the highest predictive score in *cas* genes outside intergenic regions (Fig. 3A) into the promoter-probe vector, pSEVA237R (Km^R). As a result, we evidenced the expression of the *mCherry* reporter gene by epifluorescence microscopy inspection (Fig. 3E) which confirms the presence of a regulatory region containing a constitutive alternate promoter active in *E. coli* DH5α.

Apart from the diverse transcriptional activity patterns found in native states of type I CRISPR-Cas systems, previous studies have also indicated the presence of anti-Pcas promoters in the antisense strand of *cas* genes controlling the transcription of RNA transcripts of 150–200, 220 and up to 1925 bases, respectively[46,47,50]. Knowingly, we assessed the transcriptional activity in the antisense strand of *S. xiamenensis* Sh95 type I-F1 *cas* genes by RT-PCR (Fig. 3C and D) and evidence of a long antisense transcript (> 5,2 kbp) covering *cas3f*, *cas8f1*, *cas5f1*, *cas7f1*, and *cas6f* was found (Fig. 3C and D). The absence of RT-PCR products amplification beyond the latter gene suggests it may be under control of a promoter located in the antisense strand of the leader region, which is in accordance with in-silico predictions that pointed to a single putative promoter in this locus with a high score (Fig. 3A). These results show that *S. xiamenensis* Sh95 CRISPR-Cas system is transcriptionally active and suggest that multiple rather than a single regulatory region is involved in *cas* expression.

The endogenous SxCRISPR-Cas3 enables plasmid curing

To evaluate whether the SxCRISPR-Cas3 system can recognize and process CRISPRs provided *in trans*, endogenous reprogramming experiments were performed using synthetic mini CRISPR arrays specifically designed for this system. Natural repeats and canonical spacer length (32 bp) were maintained, and a non-complementary guide was included as a control. Three mini CRISPR arrays configurations were tested, corresponding to plasmids pGanti-gfp1 (pG1), pGControl (pG2), and pGLanti-gfp1 (pG3) (Fig. 4A). The anti-gfp1 guide generates a crRNA complementary to the template strand recognizing the positions 174 to 205 of *gfpmut3* (Fig. 4B, Supplementary Table S4). The complementary guide was expressed either from the synthetic Ptac promoter (pG1) or from the native leader promoter (pG3). Introduction of these plasmids expressing crRNA guides did not cause appreciable toxicity, as bacterial growth and colony morphology were unaffected (Supplementary Fig. S3).

First, interference activity was assessed by introducing the target vector (pBKgfp, Km^R, constitutively expressing *gfpmut3*) into *S. xiamenensis* Sh95 carrying each mini CRISPR array *in trans*. The recovery of co-

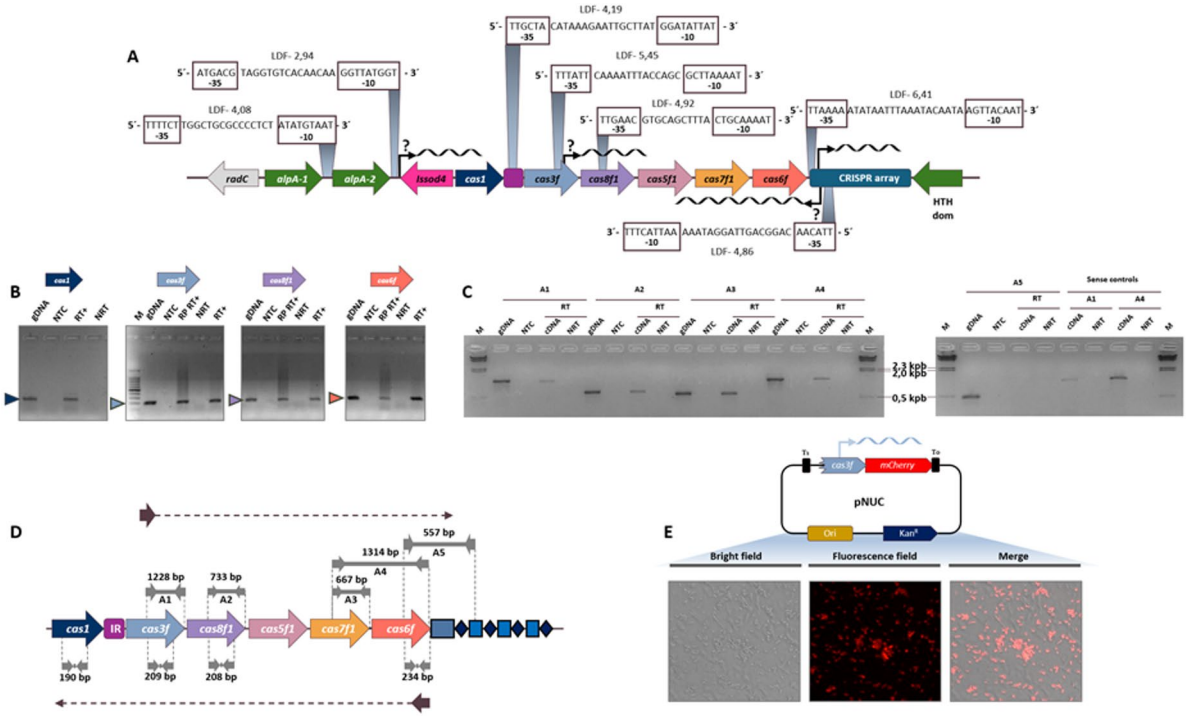

Fig. 3. Transcriptional activity of the SxCRISPR-Cas3 system. **A**) Map of promoter sequences predicted using BPROM software. The putative − 10 and − 35 boxes are depicted with rectangles and the predicted score is indicated above and below the sequences. The intergenic putative promoter sequences are shown for the three regions of SxCRISPR-Cas3: between *alpA-1* and *alpA-2*, *alpA-2* and IS *Sod4*, and between *cas1* and *cas3f*. As for intragenic promoters, only the ones with the highest predictive score (> LDF- 4) are shown for *cas3f* and *cas8f1*. The possible location of an antisense transcript promoter is represented below in 3'-5' direction. **B**) PCR products of *cas1*, *cas3f*, *cas8f1*, and *cas6f* amplified from the first strand cDNA produced using a single specific reverse primer in *cas6f* (gels were cropped to display relevant lanes and to improve clarity; migration of *cas3f*, *cas8f1* and *cas6f* products were produced in the same gel; *cas1* amplification products were run in a separated gel; all images were converted to 8 bits and inverted using FIJI before cropping). **C**) PCR products of different fragments amplified from first strand cDNA synthesis performed using a specific primer in *cas3f* that would indicate the presence of an antisense strand transcript. The amplification reaction A5 suggests that this antisense transcript does not extend outside the *cas* operon, towards the CRISPR array. Original gels are presented in Supplementary information (Supplementary Fig. S6). **D**) Schematics representing the RT-PCR amplification products of *cas* genes. Below gene arrows, small grey vector arrows represent PCR amplifications performed to assess transcription of *cas1*, *cas3f*, *cas8f1* and *cas6f*. Above the gene arrows, the grey vector arrows show the PCR products to assess antisense strand transcription. (RP RT+: first strand cDNA synthesis with random primers; RT+: first strand cDNA synthesis with specific primer; NRT: cDNA synthesis control reaction without RT; gDNA: genomic DNA, NTC: non-template control; M: molecular weight marker). **E**) Epifluorescence microscopy images of the examination of *E. coli* DH5α transformed with pNUC (the promoter-probe vector pSEVA237R into which a portion of *cas3f* ORF was cloned upstream of the *mCherry* reporter gene). The *mCherry* expression suggests that this region contains an internal constitutive functional promoter. *E. coli* DH5a carrying pNUC are shown in bright field as well as in fluorescence field with Rhodamine filter and a merge of both images is included, as indicated above (magnification: 40X).

transformants carrying both plasmids was then quantified. Using the control guide (pG2), a high number of co-transformant colonies was obtained ($10^{3.9}$ CFUs/mL) (Fig. 4C). In contrast, expression of the complementary anti-gfp1 guides under the control of either promoter led to a marked reduction in co-transformant recovery ($10^{0.33}$ and $10^{0.17}$ CFU/mL) (Fig. 4C), indicating that the system is functionally active and capable to recognize the synthetic crRNAs provided *in trans*. To quantify the interference efficiency, a plasmid loss assay was performed as previously described[54], with minor modifications, where the ratio of CFU/mL on non-selective versus selective plates was measured (NS/S). Complementary guides expressed under synthetic and native leader promoters displayed more than 10-fold and 20-fold higher efficiencies than control guides, respectively.

Then, the ability of SxCRISPR-Cas3 machinery to cure specific plasmids present in *S. xiamenensis* Sh95 strain (*S. xiamenensis* Sh95/pBKgfp, Km^R, GFP+) was evaluated by introducing the crRNA guides—expressing plasmids into colonies of *S. xiamenensis* Sh95 already harboring the target plasmid. Similar to the plasmid interference assay, the recovery of co-transformant colonies carrying complementary guides (pG1) was sharply reduced ($10^{0.33}$ CFU/mL) and exhibited approximately a 10-fold higher interference efficiency compared with the non-complementary control guide ($10^{3.1}$ CFU/mL) (pG2) (Fig. 4D).

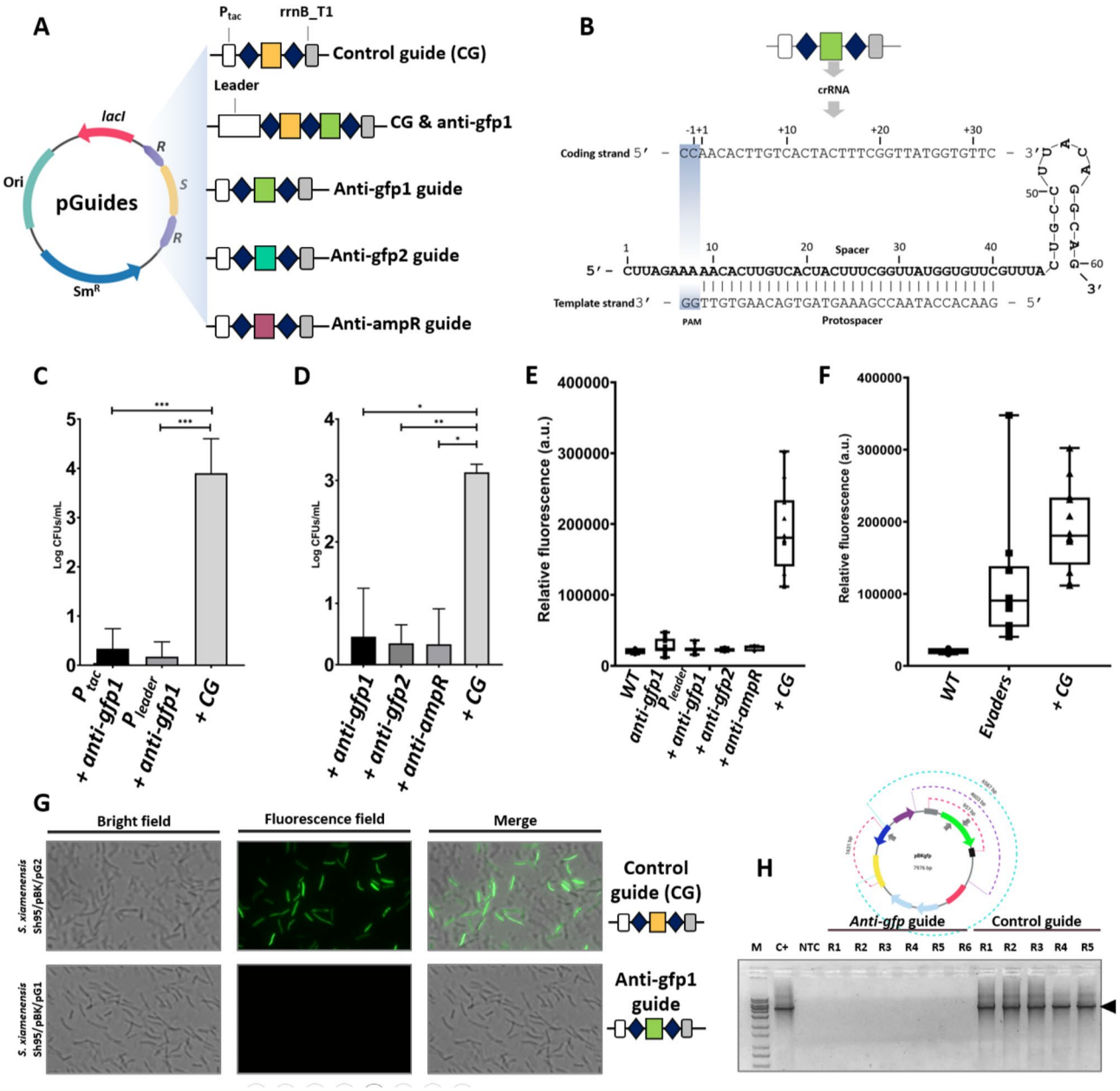

Fig. 4. Endogenous reprogramming of SxCRISPR-Cas3 leads to target plasmid elimination and re-sensitization of *S. xiamenensis* Sh95 to kanamycin. **A**) Simplified maps of the synthetic mini CRISPR arrays employed. **B**) Schematics showing the expected crRNA of anti-gfp1 after processing and interacting with the target strand of pBKgfp. Secondary structure was predicted using mFold. I-F CRISPR-Cas system's PAM is based on Gleditzsch et al., 2019[55]. **C**) Quantification of plasmid interference in *S. xiamenensis* Sh95 carrying pGanti-gfp1, pG2 (control guide, CG) or pG3 mini CRISPR arrays that were transformed with the target plasmid. A strong reduction of transformants can be observed employing targeting anti-gfp1 guides (pG1 and pG3) vs. control guides. **D**) Quantification of plasmid curing of *S. xiamenensis* Sh95 GFP + carrying the target vector pBKgfp and transformed with plasmids of either complementary anti-gfp1, anti-gfp2, and anti-ampR guides or non-complementary control guides (CG). **E**) Analysis of fluorescence values of the re-sensitized colonies (Km^S). The Km^S colonies recovered after targeting with complementary guides suffered a reduction in relative fluorescence levels measurements (a. u.). *S. xiamenensis* Sh95 wild type strain (GFP-) and transformants with the control guide (GFP+) are included as reference values. **F**) Analysis of fluorescence values in the few Km^R transformants. Relative fluorescence levels measurements (a. u.) of the survivor Km^R colonies are shown. Control guide GFP + transformants and wild type GFP- strain are included for reference. **G**) Epifluorescence microscopy images of transformants with control guide (up, GFP+) or anti-gfp guide (bottom, GFP-) are shown in bright field and fluorescence field using FITC filter (magnification 40X). **H**) PCR amplification products from the target vector of transformants with plasmids producing complementary and control guides. The gel image was cropped to show only lanes loaded with samples. Original gels are presented in supplementary information (Supplementary Fig. S7). A schematic diagram showing the PCR screening by overlapping amplifications conducted to cover the full target plasmid pBKgfp sequence is shown on top.

To further assess target recognition, two additional complementary guides were produced and evaluated to recognize positions 38–70 of *gfpmut3* (pGanti-gfp2, Sm^R) and 74–106 of the *bla*TEM, (ampicillin resistance marker) of pBKgfp (pGanti-ampR, Sm^R) (Fig. 4A). Quantification of recovered colonies revealed similar results to those observed with the anti-gfp1 guide, with a sharp reduction in transformants yielding $10^{0.35}$ and $10^{0.33}$ CFU/mL for anti-gfp2 and anti-ampR, respectively (Fig. 4D).

Examination of the few survival colonies recovered on double selective plates (LB + Km + Str) in the presence of targeting guides confirmed that these Km^R colonies retained the target pBKgfp plasmid, since it was PCR-amplified using four primer pairs covering multiple regions of its sequence (Supplementary Fig. S4). Nevertheless, these survivor colonies displayed an overall decrease in relative fluorescence levels (Fig. 4F). In contrast, analysis of colonies grown on streptomycin only plates (LB + Str), which select only for bacterial host harboring the guide-expressing plasmids, yielded target plasmid-free colonies in the presence of complementary guides. Subsequent characterization of randomly picked target plasmid-free colonies confirmed elimination of pBKgfp (Fig. 4E, G and H). Measurements of GFP fluorescence intensity in random target plasmid-free colonies showed reversal of relative fluorescence levels, comparable to the values of the wild-type *S. xiamenensis* Sh95 (Fig. 4E), and epifluorescence microscopy inspection revealed a GFP- phenotype (Fig. 4G). Analysis of controls in random co-transformant colonies using non-complementary guides yielded colonies carrying both plasmids (Fig. 4E, G and H). Finally, analysis of kanamycin susceptibility, the selective marker of pBKgfp (Km^R), showed that target plasmid-free colonies became sensitive to kanamycin (Supplementary Fig. S5), further supporting that SxCRISPR-Cas3 is functionally active and that the endogenous reprogramming strategy enables the recovery of *S. xiamenensis* Sh95 colonies cured of the target plasmid.

Discussion

This study provides an integrated characterization of the native type I-F1 CRISPR-Cas system from the clinical isolate *S. xiamenensis* Sh95. We describe its genomic organization, constitutive transcriptional activity, and an internal constitutive promoter located within *cas3f* open reading frame. Through endogenous reprogramming, plasmid interference and curing activity were observed using synthetic mini CRISPR-arrays, which demonstrates that this system is functionally active.

Comparative genomic analysis showed that genes encoding HTH- or WYL- domain-containing proteins were commonly located near *cas1* in the related I-F CRISPR-Cas systems dataset. Consistent with this observation, two copies of *alpA* were identified upstream of SxCRISPR-Cas3 locus. AlpA was previously described as involved in the excision of the cryptic P4-like prophage CP4-57 and as a component of phage-inducible chromosomal islands (PICIs)[56–59]. Furthermore, an early study suggested that CARF (CRISPR-associated Rossmann fold) and WYL domain-containing proteins accompany the genetic boundaries of CRISPR-Cas systems[60] and genes encoding proteins with HTH domains associated to casposons was described[61,62]. Moreover, WYL domain proteins are typically found with HTH domains and have also been implicated as transcriptional repressors and nucleic acid sensors of CRISPR-Cas and other defense systems[63–66] and as activators of DNA damage response by ssDNA sensing[66,67]. More recently, anti-CRISPR genes were described to localize near HTH domain-containing proteins coding genes[68–71]. The co-occurrence of these elements in the related I-F CRISPR-Cas systems could recapitulate phylogenetic relationships.

Our analysis also identified the presence of a 382 bp indel located in the intergenic region between Sh95-*cas1* and Sh95-*cas3f*. Similar sequences were found among *Shewanella* spp. and *Vibrio* spp. strains, showing a high conservation among the analyzed genomes. It was previously suggested by phylogeny analysis that *cas1* might have been horizontally transferred on a few occasions and that the genetic boundaries of CRISPR-Cas are hot spots for recombination of elements carrying *cas* genes[72,73]. The decrease in sequence identity levels immediately downstream of this locus found in the similar I-F systems that harbor this sequence, together with the absence of the highly conserved intergenic region in largely most of similar SxCRISPR-Cas3 systems, raises the question of whether this locus was lost or more recently acquired, and what biological role it may play.

Importantly, genomic rearrangements observed upstream and downstream of Sh95-*cas1* did not impair the interference functions of this system. While previous studies have described several inactivation mechanisms by anti-CRISPRs acting at post-transcriptional level[74–77], recently, ISs transpositions into CRISPR-Cas loci have also been proposed as transcriptional inhibition mechanisms[39]. Conversely, certain ISs elements, such as IS*4* and IS*Aba1*, have been described as key mobile elements that, upon transposition to a new genetic locus, can activate silent genes or enhance gene expression by providing an internal outward-facing promoter[78]. In our study, neither *alpA-2* indel, the naturally found IS*Sod4* transposition, nor the presence of *cas* antisense transcripts impaired transcription or interference functions of SxCRISPR-Cas3 system. These arrangements could have instead promoted the appearance of alternative promoter sequences, such as the one detected within Sh95-*cas3f*.

Regarding regulation, this work adds to the limited information available on transcriptional control of type I CRISPR-Cas systems, which mainly focused on I-E[51]. Thus, expression of type I-E systems was found to be regulated by H-NS in *E. coli* K-12 and *Klebsiella pneumoniae* NTUH-K2044, and dependent on growth conditions in *Salmonella enterica* serovar Typhi IMSS-1[48,50,51,73,79]. On the other hand, subtype I-F systems have been found either constitutively transcribed (in *P. atrosepticum*) or modulated in response to environmental conditions in different hosts (*P. aeruginosa* and *Serratia*sp. ATCC 39006)[53,80–82]. In addition, the induction of *P. aeruginosa* I-F system was also observed under iron availability[52]. Our findings show that the SxCRISPR-Cas3 system from *S. xiamenensis* Sh95 is transcriptionally active and constitutively expressed under standard growth conditions.

CRISPR interference has long been recognized as a potential control strategy to prevent the spread of antimicrobial resistance (AMR) genes, and the first experimental demonstration that a native CRISPR locus can prevent horizontal gene transfer by blocking plasmid conjugation and transformation into a clinical isolate of

Staphylococcus epidermidis provided early evidence for this concept[83]. This idea was very early and soon after the initial experimental evidence that CRISPR-Cas is a prokaryotic adaptive immune system[16]. Several foundational studies demonstrated the feasibility of using CRISPR-Cas systems to control bacterial pathogens and antibiotic-resistant strains as "sequence-specific antimicrobials" to selectively remove strains by sequence[84–86], to sensitize resistant bacteria to antibiotics[86,87], or to cure plasmids via CRISPR-Cas9 and type I-E[85,87]. Plasmid curing using CRISPR-Cas systems has since gained attention as means to potentially control AMR and virulence[85–93] or to remove synthetic plasmids after their use in genetic manipulations of microorganisms for industrial applications[94–96].

In this context, our results demonstrate the feasibility of SxCRISPR-Cas3 system reprogramming to allow the recovery of target plasmid-cured colonies using a simple endogenous reprogramming approach by simply adding a selective plate for the guides plasmids only supplied *in trans*. Both genome engineering tools and plasmid curing techniques are currently desired for *Shewanella* spp., as some strains hold biotechnological potential as bioremediators and bioenergy producers[12], while others, and in particular *S. xiamenensis* , rise concern over their emergence as human pathogens[285]. Considering that approximately 40% of bacteria possess a native CRISPR-Cas system[18,19], endogenous reprogramming approaches can reduce the number of plasmids needed to achieve a desired editing[21,97]. Additionally, type I-F CRISPR-Cas systems are widespread in other *Shewanella* species, such as *S. algae* , whereby this approach could be extended to related strains[5,7,29]. In particular, *S. decolorationis* and other environmental or infection-associated *Shewanella* spp. strains could benefit from this strategy for plasmid curing or other targeted applications.

At present, endogenous reprogramming of type I systems for the genetic manipulation of non-model bacteria has shown promising results across several species[84,97–106]. For instance, endogenous reprogramming of type I-F CRISPR-Cas system from *P. atrosepticum* enabled large chromosomal deletions (> 40 and > 90 kbp)[23], and similar strategies, aided by homologous templates with several features, supported targeted modifications in *Serratia sp.* ATCC 39006, multidrug-resistant *P. aeruginosa*, and *Zymomonas mobilis*[25,26,107]. In *E. coli*, inactivation of *cas3* converted the type I-E system into a programmable transcriptional repressor capable of reversible gene silencing[102]. While subtypes I-F have mainly been studied for transcriptional regulation and chromosomal editing, plasmid curing remains comparatively less explored beyond early work with I-E[85–87,94,108] and I-C CRISPR-Cas systems[109]. The re-sensitization of cured *S. xiamenensis* Sh95 colonies to kanamycin following elimination of the targeted plasmid underscores the functional activity of SxCRISPR-Cas3 and highlights its potential to aid as a tool for plasmid curing in bacteria of clinical or industrial relevance, especially for *Shewanella* spp. Although these findings confirm its interference activity, additional studies will be required to expand beyond plasmid curing, including chromosomal editing and genomic modifications leading to insertions, deletions, replacements, and nucleotide substitutions. Future work should also explore the requirements for the potential implementation of SxCRISPR-Cas3 in genomic engineering to generate diverse programmable and targeted editing outcomes.

Methods

Bacterial strains and growth conditions, DNA oligonucleotides and plasmids

Bacterial strains and plasmids used and generated in this study are listed in Supplementary tables S1 and S2, respectively. *S. xiamenensis* Sh95, *E. coli* TOP10, *E. coli* DH5α, and derivative strains used in this study (Supplementary Table S1) were propagated in Luria-Bertani medium (10 g/L tryptone, 5 g/L yeast extract and 10 g/L NaCl in dH_2O) (Britania) broth or on agar plates (1.5% wt/vol) at 37 °C under agitation at 180 rpm. *E. coli* TOP10 was used as cloning hosts. When appropriate, media were supplemented with 50 µg/mL streptomycin, 50 µg/ml kanamycin. All oligonucleotides used in this study were obtained from Genbiotech or Integrated DNA Technologies, listed in Supplementary Table S3.

In silico characterization of SxCRISPR-Cas3 system

In silico analyses were performed using the *S. xiamenensis* Sh95 genome sequence (accession number LGYY00000000.1)[41] and the complete upstream sequence obtained in this study by sequencing and subsequent assembly of contigs 66, 16, and the missing sequence. To this end, BLASTn and PSI-BLAST (version BLAST + 2.16.0, https://blast.ncbi.nlm.nih.gov/Blast.cgi) (Cas1 with 4 iterations) were initially performed to retrieve matches of highly conserved CRISPR-Cas system among *Shewanella* strains. The first comparative genomic analysis was performed against *S. decolorationis* Ni1-3 strain because this genome is fully assembled and has the highest nucleotidic as well as aminoacidic sequence identity against SxCRISPR-Cas3 system. Thus, PCR primer design of the upstream region of *cas1* of *S. xiamenensis* Sh95 was based on *S. decolorationis* Ni1-3 as reference genome. The assembled sequence was deposited in Genbank and is listed in Supplementary File 2.

Once the full upstream *cas1* region was determined, a dataset of I-F CRISPR-Cas systems related to SxCRISPR-Cas3 system was obtained by performing blastn from Sh95-*radC* to Sh95-*cas6f* against the core nucleotide database (date: 10-18-24, version BLAST + 2.15.0, https://blast.ncbi.nlm.nih.gov/Blast.cgi). The first 45 most similar sequences were retrieved (after filtering the genomes that only contained the IS*Sod4* transposed outside CRISPR-Cas systems). From this initial dataset, 19 representative genomes were selected for further analysis from each branch of a distance tree created and visualized in Blast Tree View (version 1.19.0, https://www.ncbi.nlm.nih.gov/blast/treeview/treeView.cgi). This criterion was employed to obtain different architectures of related I-F CRISPR-Cas systems. The dataset accession numbers are listed in Supplementary File 2. The analysis of CRISPR repeats and spacers sizes and number distributions, conservation and diversity, respectively, was performed employing CRISPRCasFinder (version 4.2.20, https://crisprcas.i2bc.paris-saclay.fr/CrisprCasFinder/Index)[110] and CRISPRTarget using Phage, Refseq Plasmid, and IslandViewer databases (https://crispr.otago.ac.nz/CRISPRTarget/crispr_analysis.html)[111].

The dataset of related I-F CRISPR-Cas systems that harbor the intergenic Sh95-*cas1* to Sh95-*cas3f* sequence was obtained by using the Blast all database against all isolate genomes from the Integrated Microbial Genomes & Microbiomes system (IMG/M)

(https://img.jgi.doe.gov/cgi-bin/m/main.cgi, https://img.jgi.doe.gov/cgi-bin/m/main.cgi?section=WorkspaceBlast&page=isolateform)[44,45] (date: 10-18-24), and through Genbank blastn (https://blast.ncbi.nlm.nih.gov/Blast.cgi) (date: 10-18-24). Searching the database core_nt using Blastn yielded 4 *Shewanella* genomes that were also detected employing IMG/M and *V. cholerae* O207. Further search through database wgs using Blastn was conducted for *Alteromonadales* (taxid:135622) and *Vibrionales* (taxid:135623) using *S. xiamenensis* Sh95 intergenic *cas1* to *cas3f* sequence as query. This search yielded 22 *Shewanella* spp. and 27 *Vibrios* spp. genomes that were used for multiple sequence alignments. The dataset accession numbers are listed in Supplementary Files 3 and 4. The Maximum Likelihood tree was constructed using Kimura 2-parameter model for substitutions and tested under 1000 Bootstraps replications in MEGA 11 (https://www.megasoftware.net/).

All sequences were annotated using Galaxy server (https://usegalaxy.org/) employing Prokaryotic genome annotation, Prokka (Galaxy Version 1.14.6 + galaxy1). The further nucleotide and amino acid sequence analysis were performed using the software's BLAST + 2.15.0, MEGA 11 and CLC sequence viewer (version 8.0, https://resources.qiagenbioinformatics.com/manuals/clcsequenceviewer/current/index.php? manual=Introduction_CLC_Sequence_Viewer.html) (Qiagen). For promoter sequences predictions, sequences were loaded into the online BPROM from Softberry (http://www.softberry.com/berry.phtml?topic=bprom&group=programs&subgroup=gfindb, last modification date: 24 Oct 2016) that allows the prediction of sigma 70 bacterial promoters providing the positions of detected promoters in the input sequence, along with a linear discriminant function (LDF) score for each one and weight scores for both the – 10 and – 35 elements[112,113]. The schematic figures were created using PowerPoint 2024 (https://www.microsoft.com/es-mx/microsoft-365/powerpoint).

DNA manipulations and bacterial transformations

Total DNA isolation was performed by lysozyme and proteinase K treatment followed by sodium acetate, isopropanol and ethanol precipitation[114]. Briefly, *S. xiamenensis* Sh95 or *E. coli* colonies were inoculated in 3 mL of LB broth and incubated for 18 h at 37 °C with shaking at 180 rpm. The next day, the culture was centrifuged 3 min at 12,000 x *g* and the pellet was resuspended in 200 µL of lysozyme (50 mg/mL), mixed by vortexer, and incubated at 37 °C for 15 min. Then, 250 µL of the lysis solution (TE buffer pH = 8.0 (10 mM Tris; 1 mM EDTA), 25 µL 10% SDS, and 4 µL of Proteinase K 20 mg/ml) were added. Again, it was homogenized by vortexer and incubated at 37 °C for one hour. Next, 1 µL of DNase-free RNase A (10 mg/mL) was added and incubated under the same conditions for 15 min. Each tube was immediately placed on ice for 5 min, then 285 µL of cold 3 M sodium acetate was added and shaken by inversion. Samples were further incubated for 30 min on ice and then centrifuged at 12,000 xg for 15 min. The supernatant was transferred to a new tube with 500 µL of cold isopropanol and gently inverted. The previous centrifugation was repeated, and the aqueous phase was removed. The precipitate was washed with 900 µL of cold 90% ethanol, centrifuged at 12,000 x g for 2 min, and the aqueous phase was carefully removed. Once the evaporation of residual ethanol was confirmed, the precipitated DNA was recovered in 100 µL of MilliQ Ultrapure H_2O and incubated at 55 °C for 10 min. The presence and integrity of the genomic DNA obtained was verified by electrophoretic migration and was quantified by nanodrop spectrophotometry (Nano-500).

E. coli electrocompetent cells were prepared using the protocol described by Sambrook & Russell (2001)[114]. *S. xiamenensis* Sh95 competent cells were prepared as previously described[115]. Briefly, a colony of the bacteria to be transformed was taken, 6 mL of LB medium was inoculated and incubated at 37 °C for 18 h with shaking at 200 rpm. The next day, the culture was centrifuged at 12,000 x g for 3 min, the supernatant was discarded, and the pellet was resuspended in 1 mL of 300 mM sucrose (at room temperature). The cells were centrifuged at 12,000 x*g* for 3 min and the procedure was repeated 3 times. Finally, the pellet was resuspended in 200 µL of 300 mM sucrose. Competent cells were transformed with plasmids by electroporation (Gene Pulser, Bio-Rad) using 0.1-cm gap cuvettes with 2.5 kV/cm, 200 Ω, 25 µF. Immediately, 1 mL of LB broth or SOB was added to the transformed samples and allowed to recover for 1 h at 37 °C 180 rpm until plated on the surface of suitable selection plates.

Construction of plasmids

The clinical isolate *S. xiamenensis* Sh95 genomic DNA was used as a template to amplify the *cas3f* gene. This product was ligated into the pRSFDuet-1 (Km^R) vector MCS-1 using BamHI (New England Biolabs) restriction endonuclease cut sites and T4 DNA ligase (Promega) to obtain the plasmid pI20. The plasmid was confirmed by restriction digestion patterns and sequenced using BTseq (Celemics). In a second step, subcloning of a *cas3f* fragment (positions 844–3486) was carried out from the recombinant plasmid pI20 generated into the promoterless pSEVA237R (Km^R, mCherry) MCS using BamHI (New England Biolabs) and EcoRI (New England Biolabs) restriction endonuclease cut sites. Both double digested plasmids were gel purified prior to the ligation reaction using T4 DNA ligase (Promega) of the linearized vector pSEVA237R and the 2644 bp band corresponding to *cas3f* positions 844–3486. Thus, pNUC plasmid was obtained. The plasmid obtained was confirmed by restriction digestion patterns and by Sanger sequencing (Macrogen). Full plasmid sequences are available in GenBank under accession numbers listed in Supplementary File 1.

Synthetic mini CRISPR arrays were specifically designed for recognition by the SxCRISPR-Cas3 system machinery of *S. xiamenensis* Sh95 (Supplementary Table S4) based on the following criteria. The synthetic crRNA guides are under control of the native leader of the CRISPR array of *S. xiamenensis* Sh95 and the complementary guide is placed on the second position of the array (pG3), or synthetic crRNA guides are under the strong Ptac promoter where both complementary and control guide are located on the first position (pG1 and pG2). Guides consist of a 32 bp spacer sequence flanked by the native repeats of the SxCRISPR-Cas3 system.

The rrnBT1 transcriptional terminator was included following the last repeat of the array. The mini CRISPR arrays designed were synthesized and cloned into pCDFDuet (Sm^R) (Genescript) producing the plasmids pG1 (anti-gfp1 guide under Ptac), pG2 (control guide under Ptac) and pG3 (control guide in first position, anti-gfp1 guide in second position, under control of leader). In the pG2 plasmid, the sequence incorporated is not complementary to any other sequence as a control guide that was designed based on the sequenced genomes of *E. coli* BL21(DE3) and *S. xiamenensis* Sh95. In addition, a modular structure was designed and included in pG2 to allow the cloning of new guides by the Golden Gate Assembly method through BsaI digestion and insertion of annealed oligonucleotides. New guides, pGanti-gfp2 and pGanti-ampR, were generated using this modular backbone and strategy. The procedures were confirmed by Sanger sequencing (Macrogen) and full plasmid sequences are available in GenBank under accession numbers listed in Supplementary File 1. The specificity for all designed guides was tested using BLASTn with parameters adequate for short input sequences: word size 7; match/missmatch score 1, -3; gap costs 5, 2 against plasmids sequences and genome sequences employed.

Endogenous reprogramming assays

Plasmid interference assays

Electrocompetent cells of previously constructed *S. xiamenensis* Sh95/pG1 (Sm^R), *S. xiamenensis* Sh95/pG2 (Sm^R), and *S. xiamenensis* Sh95/pG3 (Sm^R) were transformed with target plasmid pBKgfp by electroporation as previously described. After recovery, an aliquot of each bacterial suspension was taken to make serial dilutions with dilution factors of 10. Next, 100 µL of each dilution and 100 µL of the undiluted suspension were plated on selective and non-selective plates for the target plasmid, pBKgfp. A plasmid loss assay described by Xiao & Ke (2019)[54] was performed with some modifications. The selective plates corresponded to LB supplemented with Sm 50 µg/mL and Km 50 µg/mL, while the non-selective plates were from LB supplemented with Sm 50 µg/mL. They were incubated overnight at 37 °C and, the next day, CFUs/mL counts were performed on selective and non-selective plates. Experiments were performed in triplicate. The interference efficiency by CRISPR was determined as the number of CFUs/mL in non-selective plates vs. selective (NS/S).

Plasmid curing assays

S. xiamenensis Sh95/pBKgfp was constructed and then transformed with pG1(Sm^R), pG2(Sm^R), pGanti-gfp2 (Sm^R), or pGanti-ampR (Sm^R) in a second step. After recovery, an aliquot of each bacterial suspension was taken to make serial dilutions with dilution factors of 10. Next, 100 µL of each dilution and 100 µL of the undiluted suspension were plated on selective and non-selective plates for the target plasmid, pBKgfp. A plasmid loss assay described by Xiao & Ke (2019)[54] was performed with some modifications. The selective plates corresponded to LB supplemented with Km 50 µg/mL and Str 50 µg/mL, while the non-selective plates were from LB supplemented with kanamycin 50 µg/mL. An additional plate was included in the assay supplemented with 50 µg/mL Str (selective only for the plasmid that enters in the last step, pG1, pG2, pGanti-gfp2 or pGanti-ampR). They were incubated overnight at 37 °C and, the next day, CFU/mL counts were performed on selective and non-selective plates. Experiments were performed in triplicate. The interference efficiency by CRISPR is determined as the number of CFU/mL in non-selective plates vs. selective. To confirm re-sensitized *S. xiamenensis* Sh95, survivor colonies were randomly picked and re-streaked on appropriate selective plates and incubated overnight at 37 C.

PCR screenings

Screening of target plasmid under SxCRISPR-Cas3 system reprogramming was carried out by overlapping PCR amplification of the whole vector sequence employing 4 sets of primers. PCR products sizes were analyzed according to their electrophoretic migration profile.

Fluorescence microscopy

Aliquots of cell culture or small amounts of cells growing in solid media were collected with a sterile tip and suspended in drops of 0,85% NaCl solution placed on microscope glass slides and a coverslip was gently placed from 45° on the suspension. Unless otherwise specified in the text, all samples were observed under Olympus BX50 with Olympus PlanApo N 60x and 40x oil objective and 460–490 nm excitation filter. Images were obtained with OLYMPUS cellSens Entry 1.18 software and processed by FIJI/ImageJ 1.54p.

Fluorimetry

20 µL of ON cultures were deposited as drops on top of appropriate LB agar selective plates. When all liquid was absorbed, the plates were incubated overnight at 37 °C. The next day, cells were collected using a sterile microbiology loop and resuspended in 1X PBS (pH 7,4). To eliminate dead cells, free fluorescent proteins and detritus, cells were spin down 16000x*g* for 2 min and washed once with PBS. Cells were resuspended in fresh PBS to measure OD_{600nm}, all samples were diluted in fresh PBS to reach an adjusted value of OD_{600nm} 0,7 and relative fluorescence measures were gathered using Nano500 with 460 ± 20 nm excitation and 525 to 570 nm emission filters. For all samples, relative fluorescence values were corrected by subtracting the reading for PBS only solution.

RNA extraction for transcriptional analysis of SxCRISPR-Cas3

Extraction of total bacterial RNA from *S. xiamenensis* Sh95 was performed using Trizol reagent (Invitrogen). Briefly, pellets of 1 ml of bacterial culture with an OD_{600nm} of 0.8 or 750 uL of overnight cultures were resuspended with 500 µl of Trizol and incubated for 5 min at room temperature. Then, 100 µl of chloroform was added to each sample, shaken vigorously for 15 s, and incubated for 2–3 min at room temperature. Next, samples were centrifuged for 15 min at 4 °C at a speed of 12,000 xg and the aqueous phase was transferred to a new tube. RNA was precipitated from each sample by adding 250 µl of isopropanol and incubating for 10 min at room

temperature. Then, the samples were centrifuged again at 4 °C for 10 min at 12,000 x g. The RNA was washed with 75% ethanol and centrifuged for 5 min at 4 °C at a speed of 7,500 x g. Finally, the sRNAs were resuspended in 50 µl of ultrapure diethylpyrocarbonate (DEPC) treated water, free of ribonucleases, and incubated at 55 °C for 10 min. To eliminate any possible residual gDNA from the extraction, all RNAs were then treated with 2 units of the enzyme RQ1 RNase-Free DNase (Promega, Madison, USA) for 2 h at 37 C, which was then inactivated with the addition of 2 units of the stop solution at 65 °C for 10 min, following manufacturer instructions. The integrity and high quality of the RNA obtained was assessed by electrophoretic migration, by negative control PCR amplifications reactions using 1 µl of the extracted total RNA as a template and quantified by nanodrop (Nano500). The synthesis of complementary DNA (cDNA) was carried out from 1 µg of high-quality total RNA, treated with DNase I (Promega). The absence of genomic DNA was confirmed by control PCR amplifications of the genes of interest. Then, the first strand of cDNA was synthesized using random primers or specific primers, as appropriate. In the first step, total RNA and primers were denatured for 5 min at 70 °C, followed by immediate incubation for 4 min at 4 °C. 200 units of the M-MLV reverse transcriptase enzyme (Promega) were used and the reaction was set up following the manufacturer's specifications. The reaction was carried out in a thermocycler (Multigene™, Labnet) at 42 °C for 120 min. Subsequently, following manufacturer instructions, all samples were heat-inactivated by incubation at 70 °C for 15 min.

Data availability

All data generated or analysed during this study are included in this published article (and its Supplementary Information files). The datasets generated and/or analysed during the current study are available in the GenBank repository, accession numbers are listed in Supplementary Files 1 to 4.

Received: 14 April 2025; Accepted: 29 December 2025
Published online: 27 January 2026

References

1. Fredrickson, J. K. et al. Towards environmental systems biology of *Shewanella*. *Nature Reviews Microbiology* **6**, 592–603 Preprint at https://doi.org/10.1038/nrmicro1947 (2008).
2. Gorby, Y. A. *et al. Electrically Conductive Bacterial Nanowires Produced by Shewanella Oneidensis Strain MR-1 and Other Microorganisms*. https://doi.org/10.1073/pnas.060451710 (2006).
3. Ji, Q. et al. Removal of water-insoluble Sudan dyes by *Shewanella oneidensis* MR-1. *Bioresour Technol.* **114**, 144–148 (2012).
4. Logan, B. E., Rossi, R., Ragab, A. & Saikaly, P. E. Electroactive microorganisms in bioelectrochemical systems. *Nature Reviews Microbiology* **17**, 307–319 Preprint at https://doi.org/10.1038/s41579-019-0173-x (2019).
5. Cerbino, G. N. et al. Comparative genome analysis of the genus *Shewanella* unravels the association of key genetic traits with known and potential pathogenic lineages. *Front Microbiol* **14**, (2023).
6. Ng, W. W. S., Shum, H. P., To, K. K. W. & Sridhar, S. Emerging infections due to *Shewanella* spp.: A case series of 128 cases over 10 years. *Front Med. (Lausanne)* **9**, 1–8 (2022).
7. Wang, A., Hibdon, M., Desaraju, C. & Liu-Young, G. Treatment and management of *Shewanella algae* necrotizing cellulitis. *Cureus* https://doi.org/10.7759/cureus.73680 (2024).
8. Yu, K., Huang, Z., Xiao, Y. & Wang, D. *Shewanella* infection in humans: Epidemiology, clinical features and pathogenicity. *Virulence* **13**, 1515–1532 Preprint at https://doi.org/10.1080/21505594.2022.2117831 (2022).
9. Yousfi, K., Bekal, S., Usongo, V. & Touati, A. Current trends of human infections and antibiotic resistance of the genus *Shewanella*. *European Journal of Clinical Microbiology and Infectious Diseases* **36**, 1353–1362 Preprint at https://doi.org/10.1007/s10096-017-2962-3 (2017).
10. Corts, A., Thomason, L. C., Costantino, N. & Court, D. L. Recombineering in Non-Model bacteria. *Curr Protoc* **2**, 1–58 (2022).
11. Chen, Y., Cheng, M., Song, H. & Cao, Y. Type I-F CRISPR-PAIR platform for multi-mode regulation to boost extracellular electron transfer in *Shewanella oneidensis*. *iScience* **25**, 1–16 (2022).
12. Corts, A. D., Thomason, L. C., Gill, R. T. & Gralnick, J. A. A new recombineering system for precise genome-editing in *Shewanella oneidensis* strain MR-1 using single-stranded oligonucleotides. *Sci Rep* **9**, 1–10 (2019).
13. Yusuke Suzuki, A. Kazuya Watanabe. CRISPR/Cas9-mediated genome editing of *Shewanella oneidensis* MR-1 using a broad host-range pBBR1-based plasmid. *J. Gen. Appl. Microbiol.* **13**, 1–2 (2019).
14. Makarova, K. S., Grishin, N. V., Shabalina, S. A., Wolf, Y. I. & Koonin, E. V. A putative RNA-interference-based immune system in prokaryotes: Computational analysis of the predicted enzymatic machinery, functional analogies with eukaryotic RNAi, and hypothetical mechanisms of action. *Biology Direct* vol. 1 Preprint at https://doi.org/10.1186/1745-6150-1-7 (2006).
15. Mojica, F. J. M., Díez-Villaseñor, C., García-Martínez, J. & Soria, E. Intervening sequences of regularly spaced prokaryotic repeats derive from foreign genetic elements. *J. Mol. Evol.* **60**, 174–182 (2005).
16. Barrangou R et al. CRISPR Provides Acquired Resistance Against Viruses in Prokaryotes.Science **315**, 1709–1712 (2007).
17. Mayo-Muñoz, D., Pinilla-Redondo, R., Birkholz, N. & Fineran, P. C. A host of armor: Prokaryotic immune strategies against mobile genetic elements. *Cell Reports* **42**, Preprint at https://doi.org/10.1016/j.celrep.2023.112672 (2023).
18. Makarova, K. S. et al. Evolutionary classification of CRISPR–Cas systems: a burst of class 2 and derived variants. *Nature Reviews Microbiology* **18**, 67–83 Preprint at https://doi.org/10.1038/s41579-019-0299-x (2020).
19. Ishino, Y., Krupovic, M. & Forterre, P. History of CRISPR-Cas from encounter with a mysterious repeated sequence to genome editing technology. *J Bacteriol* **200**, 1–17 (2018).
20. Liu, T. Y. & Doudna, J. A. Chemistry of Class 1 CRISPR-Cas effectors: Binding, editing, and regulation. *Journal of Biological Chemistry* **295**, 14473–14487 Preprint at https://doi.org/10.1074/jbc.REV120.007034 (2020).
21. Zheng, Y. et al. Endogenous Type I CRISPR-Cas: From Foreign DNA Defense to Prokaryotic Engineering. *Frontiers in Bioengineering and Biotechnology* **8**, Preprint at https://doi.org/10.3389/fbioe.2020.00062 (2020).
22. Liu, Z. et al. Endogenous CRISPR-Cas mediated in situ genome editing: State-of-the-art and the road ahead for engineering prokaryotes. *Biotechnology Advances* **68**, Preprint at https://doi.org/10.1016/j.biotechadv.2023.108241 (2023).
23. Vercoe, R. B. et al. Cytotoxic chromosomal targeting by CRISPR/Cas systems can reshape bacterial genomes and expel or remodel pathogenicity Islands. *PLoS Genet* **9**, 1–13 (2013).
24. Rollins, M. F., Schuman, J. T., Paulus, K., Bukhari, H. S. T. & Wiedenheft, B. Mechanism of foreign DNA recognition by a CRISPR RNA-guided surveillance complex from *Pseudomonas aeruginosa*. *Nucleic Acids Res.* **43**, 2216–2222 (2015).
25. Hampton, H. G. et al. CRISPR-Cas gene-editing reveals RsmA and RsmC act through FlhDC to repress the SdhE flavinylation factor and control motility and prodigiosin production in *Serratia*. *Microbiol. (United Kingdom)*. **162**, 1047–1058 (2016).

26. Xu, Z. et al. Native CRISPR-Cas-Mediated genome editing enables dissecting and sensitizing clinical Multidrug-Resistant *P. aeruginosa*. *Cell. Rep.* **29**, 1707–1717e3 (2019).
27. Tuminauskaite, D. et al. DNA interference is controlled by R-loop length in a type I-F1 CRISPR-Cas system. *BMC Biol* **18**, 1–16 (2020).
28. Wang, J. H., Tseng, S. Y. & Tung, K. C. Genomic investigation of emerging zoonotic pathogen *Shewanella xiamenensis*. *Tzu Chi Med. J.* **32**, 162–166 (2020).
29. Wang, J. H. et al. Characterization of CRISPR-Cas Systems in *Shewanella algae* and *Shewanella haliotis*: Insights into the Adaptation and Survival of Marine Pathogens. *Pathogens* **13** (6), 439 (2024).
30. Lin, W. Q. et al. Efficient enhancement of extracellular electron transfer in *Shewanella oneidensis* MR-1 via CRISPR-Mediated transposase technology. *ACS Synth. Biol.* **13**, 1941–1951 (2024).
31. Cheng, L. et al. Developing a base-editing system to expand the carbon source utilization spectra of *Shewanella oneidensis* MR-1 for enhanced pollutant degradation. *Biotechnol. Bioeng.* **117**, 2389–2400 (2020).
32. Cao, Y., Li, X., Li, F. & Song, H. CRISPRi-sRNA: Transcriptional-Translational regulation of extracellular electron transfer in *Shewanella oneidensis*. *ACS Synth. Biol.* **6**, 1679–1690 (2017).
33. Corts, A. D., Thomason, L. C., Gill, R. T. & Gralnick, J. A. Efficient and precise genome editing in *Shewanella* with recombineering and CRISPR/Cas9-Mediated Counter-Selection. *ACS Synth. Biol.* **8**, 1877–1889 (2019).
34. Chen, Y. et al. Development of whole Genome-Scale base editing toolbox to promote efficiency of extracellular electron transfer in *Shewanella oneidensis* MR-1. *Adv Biol* **6**, (2022).
35. Chen, Y. et al. Highly efficient multiplex base editing: One-shot deactivation of eight genes in *Shewanella oneidensis* MR-1. *Synth. Syst. Biotechnol.* **8**, 1–10 (2023).
36. Dwarakanath, S. et al. Interference activity of a minimal type I CRISPR-Cas system from *Shewanella putrefaciens*. *Nucleic Acids Res.* **43**, 8913–8923 (2015).
37. Gleditzsch, D. et al. Modulating the cascade architecture of a minimal type I-F CRISPR-Cas system. *Nucleic Acids Res.* **44**, 5872–5882 (2016).
38. Wang, X. et al. Type I-F CRISPR-associated transposons contribute to genomic plasticity in *Shewanella* and mediate efficient programmable DNA integration. *Microb Genom* **11**, 1–15 (2025).
39. Sheng, Y. et al. Insertion sequence transposition inactivates CRISPR-Cas immunity. *Nat Commun* **14**, 1–15 (2023).
40. Hennig, S. & Ziebuhr, W. Characterization of the transposase encoded by IS*256*, the prototype of a major family of bacterial insertion sequence elements. *J. Bacteriol.* **192**, 4153–4163 (2010).
41. Parmeciano Di Noto, G., Jara, E., Iriarte, A., Centrón, D. & Quiroga, C. Genome analysis of a clinical isolate of Shewanella sp. Uncovered an active hybrid integrative and conjugative element carrying an integron platform inserted in a novel genomic locus. *Microbiol. (United Kingdom)*. **162**, 1335–1345 (2016).
42. Nuñez, J. K., Bai, L., Harrington, L. B., Hinder, T. L. & Doudna, J. A. CRISPR immunological memory requires a host factor for specificity. *Mol. Cell.* **62**, 824–833 (2016).
43. Pausch, P. et al. Structural variation of type I-F CRISPR RNA guided DNA surveillance. *Mol. Cell.* **67**, 622–632e4 (2017).
44. Chen, I. M. A. et al. The IMG/M data management and analysis system v.7: content updates and new features. *Nucleic Acids Res.* **51**, D723–D732 (2023).
45. Mukherjee, S. et al. Twenty-five years of genomes online database (GOLD): data updates and new features in v.9. *Nucleic Acids Res.* **51**, D957–D963 (2023).
46. Pul, Ü. et al. Identification and characterization of E. coli CRISPR-Cas promoters and their silencing by H-NS. *Mol. Microbiol.* **75**, 1495–1512 (2010).
47. Westra, E. R. et al. H-NS-mediated repression of CRISPR-based immunity in Escherichia coli K12 can be relieved by the transcription activator LeuO. *Mol. Microbiol.* **77**, 1380–1393 (2010).
48. Medina-Aparicio, L. et al. The CRISPR/Cas immune system is an Operon regulated by LeuO, H-NS, and leucine-responsive regulatory protein in *Salmonella enterica* serovar Typhi. *J. Bacteriol.* **193**, 2396–2407 (2011).
49. Yang, C. D. et al. P. CRP represses the CRISPR/Cas system in *Escherichia coli:* evidence that endogenous CRISPR spacers impede phage P1 replication. *Mol. Microbiol.* **92**, 1072–1091 (2014).
50. Medina-Aparicio, L. et al. CRISPR-Cas system presents multiple transcriptional units including antisense RNAs that are expressed in minimal medium and upregulated by pH in *Salmonella enterica* serovar Typhi. *Microbiol. (United Kingdom)*. **163**, 253–265 (2017).
51. Xue, C. & Sashital, D. G. Mechanisms of type I-E and I-F CRISPR-Cas systems in Enterobacteriaceae. *EcoSal Plus* **8**, 1–24 (2019).
52. Ahator, S., Dela, Jianhe, W. & Zhang, L. H. The ECF sigma factor PvdS regulates the type I-F CRISPR-Cas system in *Pseudomonas aeruginosa*. Preprint at https://doi.org/10.1101/2020.01.31.929752 (2020).
53. Patterson, A. G., Chang, J. T., Taylor, C. & Fineran, P. C. Regulation of the type I-F CRISPR-Cas system by CRP-cAMP and GalM controls spacer acquisition and interference. *Nucleic Acids Res.* **43**, 6038–6048 (2015).
54. Xiao, Y. & Ke, A. Reconstitution and biochemical characterization of ribonucleoprotein complexes in type I-E CRISPR–Cas systems. in *Methods in Enzymology* **616** 27–41 (Academic Press Inc., (2019).
55. Gleditzsch, D. et al. PAM identification by CRISPR-Cas effector complexes: diversified mechanisms and structures. *RNA Biology* **16**, 504–517 Preprint at https://doi.org/10.1080/15476286.2018.1504546 (2019).
56. Kirby, J. E., Trempy, J. E., & Gottesman, S. Excision of a P4-like cryptic prophage leads to Alp protease expression in *Escherichia coli*. *Journal of bacteriology*, **176**(7), 2068–2081. https://doi.org/10.1128/jb.176.7.2068-2081.1994 (1994).
57. Fillol-Salom, A. et al. Phage-inducible chromosomal Islands are ubiquitous within the bacterial universe. *ISME J.* **12**, 2114–2128 (2018).
58. Ibarra-Chávez, R., Hansen, M. F., Pinilla-Redondo, R., Seed, K. D. & Trivedi, U. Phage satellites and their emerging applications in biotechnology. *FEMS Microbiology Reviews* **45**, Preprint at https://doi.org/10.1093/femsre/fuab031 (2021).
59. Barcia-Cruz, R. et al. Phage-inducible chromosomal minimalist Islands (PICMIs), a novel family of small marine satellites of virulent phages. *Nat Commun* **15**, 1–13 (2024).
60. Makarova, K. S., Anantharaman, V., Grishin, N. V., Koonin, E. V. & Aravind, L. CARF and WYL domains: Ligand-binding regulators of prokaryotic defense systems. *Front Genet* **5**, 1–9 (2014).
61. Krupovic, M., Béguin, P. & Koonin, E. V. Casposons: mobile genetic elements that gave rise to the CRISPR-Cas adaptation machinery. *Current Opinion in Microbiology* **38**, 36–43 Preprint at https://doi.org/10.1016/j.mib.2017.04.004 (2017).
62. Smaruj, P. & Kieliszek, M. Casposons – silent heroes of the crispr-cas systems evolutionary history. *EXCLI Journal* **22**, 70–83 Preprint at https://doi.org/10.17179/excli2022-5581 (2023).
63. Hein, S., Scholz, I., Björn, V. & Hess, W. R. Adaptation and modification of three CRISPR loci in two closely related cyanobacteria. *RNA Biol.* **10**, 852–864 (2013).
64. Picton, D. M. et al. A widespread family of WYL-domain transcriptional regulators co-localizes with diverse phage defence systems and Islands. *Nucleic Acids Res.* **50**, 5191–5207 (2022).
65. Keller, L. M. & Weber-Ban, E. An emerging class of nucleic acid-sensing regulators in bacteria: WYL domain-containing proteins. *Curr Opin. Microbiol* **74**, 1–11 (2023).
66. Schumacher, M. A. et al. Structure of the WYL-domain containing transcription activator, DriD, in complex with ssDNA effector and DNA target site. *Nucleic Acids Res.* **52**, 1435–1449 (2024).

67. Gozzi, K., Salinas, R., Nguyen, V. D., Laub, M. T. & Schumacher, M. A. SsDNA is an allosteric regulator of the *C. crescentus* SOS-independent DNA damage response transcription activator, DriD. *Genes Dev.* **36**, 618–633 (2022).
68. Birkholz, N., Fagerlund, R. D., Smith, L. M., Jackson, S. A. & Fineran, P. C. The autoregulator Aca2 mediates anti-CRISPR repression. *Nucleic Acids Res.* **47**, 9658–9665 (2019).
69. Lee, S. Y., Birkholz, N., Fineran, P. C. & Park, H. H. Molecular basis of anti-CRISPR Operon repression by Aca10. *Nucleic Acids Res.* **50**, 8919–8928 (2022).
70. Stanley, S. Y. et al. Anti-CRISPR-Associated proteins are crucial repressors of Anti-CRISPR transcription. *Cell* **178**, 1452–1464e13 (2019).
71. Usher, B. et al. Crystal structure of the anti-CRISPR repressor Aca2. *J Struct. Biol* **213**, 1–8 (2021).
72. Godde, J. S. & Bickerton, A. The repetitive DNA elements called crisprs and their associated genes: evidence of horizontal transfer among prokaryotes. *J. Mol. Evol.* **62**, 718–729 (2006).
73. Touchon, M. & Rocha, E. P. C. The small, slow and specialized CRISPR and anti-CRISPR of *Escherichia* and *Salmonella*. *PLoS One* **5**, 1–14 (2010).
74. Pawluk, A., Davidson, A. R. & Maxwell, K. L. Anti-CRISPR: Discovery, mechanism and function. *Nat. Rev. Microbiol.* **16**, 12–17 (2018).
75. Yang, L., Zhang, Y., Yin, P. & Feng, Y. Structural insights into the inactivation of the type I-F CRISPR-Cas system by anti-CRISPR proteins. *RNA Biology* **18**, 562–573 Preprint at https://doi.org/10.1080/15476286.2021.1985347 (2021).
76. Camara-Wilpert, S. et al. Bacteriophages suppress CRISPR–Cas immunity using RNA-based anti-CRISPRs. *Nature* **623**, 601–607 (2023).
77. Wimmer, F. et al. Interrogating two extensively self-targeting type I CRISPR-Cas systems in *Xanthomonas albilineans* reveals distinct anti-CRISPR proteins that block DNA degradation. *Nucleic Acids Res.* **52**, 769–783 (2024).
78. Lipszyc, A., Szuplewska, M. & Bartosik, D. How Do Transposable Elements Activate Expression of Transcriptionally Silent Antibiotic Resistance Genes? *International Journal of Molecular Sciences* **23**, Preprint at https://doi.org/10.3390/ijms23158063 (2022).
79. Lin, T. L. et al. Imipenem represses CRISPR-Cas interference of DNA acquisition through H-NS stimulation in *Klebsiella pneumoniae*. *Sci Rep* **6**, 1–10 (2016).
80. Patterson, A. G. et al. Quorum sensing controls adaptive immunity through the regulation of multiple CRISPR-Cas systems. *Mol. Cell.* **64**, 1102–1108 (2016).
81. Høyland-Kroghsbo, N. M. et al. Quorum sensing controls the *Pseudomonas aeruginosa* CRISPR-Cas adaptive immune system. *Proc. Natl. Acad. Sci. U S A.* **114**, 131–135 (2017).
82. Høyland-Kroghsbo, N. M., Muñoz, K. A. & Bassler, B. L. Temperature, by controlling growth rate, regulates CRISPR-Cas activity in *Pseudomonas aeruginosa*. *mBio* 9, 1–12 (2018).
83. Marraffini, L. A. & Sontheimer, E. J. CRISPR interference limits horizontal gene transfer in *Staphylococci* by targeting DNA. *Sci. (1979).* **322**, 1843–1845 (2008).
84. Gomaa, A. A. et al. Programmable removal of bacterial strains by use of genome- targeting CRISPR-cas systems. *mBio* **5**, 1–9 (2014).
85. Bikard, D. et al. Exploiting CRISPR-cas nucleases to produce sequence-specific antimicrobials. *Nat. Biotechnol.* **32**, 1146–1150 (2014).
86. Citorik, R. J., Mimee, M. & Lu, T. K. Sequence-specific antimicrobials using efficiently delivered RNA-guided nucleases. *Nat. Biotechnol.* **32**, 1141–1145 (2014).
87. Yosef, I., Manor, M., Kiro, R. & Qimron, U. Temperate and lytic bacteriophages programmed to sensitize and kill antibiotic-resistant bacteria. *Proc. Natl. Acad. Sci. U S A.* **112**, 7267–7272 (2015).
88. Bikard, D. & Barrangou, R. Using CRISPR-Cas systems as antimicrobials. *Current Opinion in Microbiology* **37**, 155–160 Preprint at https://doi.org/10.1016/j.mib.2017.08.005 (2017).
89. Duan, C., Cao, H., Zhang, L. H. & Xu, Z. Harnessing the CRISPR-Cas Systems to Combat Antimicrobial Resistance. *Frontiers in Microbiology* **12**, Preprint at https://doi.org/10.3389/fmicb.2021.716064 (2021).
90. Hao, M. et al. CRISPR-Cas9-Mediated Carbapenemase Gene and Plasmid Curing in Carbapenem-Resistant *Enterobacteriaceae*. *Antimicrobial agents and chemotherapy*, **64**(9), 1–10 e00843–20. https://doi.org/10.1128/AAC.00843-20 (2020).
91. Walker-Sünderhauf, D. et al. Removal of AMR plasmids using a mobile, broad host-range CRISPR-Cas9 delivery tool. *Microbiology (United Kingdom)* **169**, 1–14 (2023).
92. Wang, X. et al. Application of CRISPR/Cas9 system for plasmid elimination and bacterial killing of *Bacillus cereus* group strains. *Front Microbiol* **12**, 1–17 (2021).
93. Zhou, Y. et al. Exploiting a conjugative endogenous CRISPR-Cas3 system to tackle multidrug-resistant *Klebsiella pneumoniae*. *EBioMedicine* **88**, 1–16 (2023).
94. Caliando, B. J. & Voigt, C. A. Targeted DNA degradation using a CRISPR device stably carried in the host genome. *Nat Commun* **6**, 1–10 (2015).
95. Jervis, A. J. et al. A plasmid toolset for CRISPR-mediated genome editing and CRISPRi gene regulation in *Escherichia coli*. *Microb. Biotechnol.* **14**, 1120–1129 (2021).
96. Lauritsen, I., Porse, A., Sommer, M. O. A. & Nørholm, M. H. H. A versatile one-step CRISPR-Cas9 based approach to plasmid-curing. *Microb Cell. Fact* **16**, 1–10 (2017).
97. Yao, S. et al. Harnessing the native type I-F CRISPR-Cas system of acinetobacter baumannii for genome editing and gene repression. *Int J. Antimicrob. Agents* **62**, (2023).
98. Baker, P. L. et al. Using the endogenous CRISPR-Cas system of *Heliobacterium modesticaldum* to Delete the photochemical reaction center core subunit gene. *Appl Environ. Microbiol* **85**, 1–18 (2019).
99. Cañez, C., Selle, K., Goh, Y. J. & Barrangou, R. Outcomes and characterization of chromosomal self-targeting by native CRISPR-Cas systems in *Streptococcus thermophilus*. *FEMS Microbiol. Lett* **366**, (2019).
100. Hidalgo-Cantabrana, C., Goh, Y. J., Pan, M., Sanozky-Dawes, R. & Barrangou, R. Genome editing using the endogenous type I CRISPR-Cas system in *Lactobacillus crispatus*. *Proc. Natl. Acad. Sci. U S A.* **116**, 15774–15783 (2019).
101. Li, Y. et al. Harnessing type I and type III CRISPR-Cas systems for genome editing. *Nucleic Acids Res* **44**, 1–12 (2015).
102. Luo, M. L., Mullis, A. S., Leenay, R. T. & Beisel, C. L. Repurposing endogenous type I CRISPR-Cas systems for programmable gene repression. *Nucleic Acids Res.* **43**, 674–681 (2015).
103. Maikova, A., Kreis, V., Boutserin, A., Severinov, K. & Soutourina, O. Using an endogenous CRISPR-Cas system for genome editing in the human pathogen *Clostridium difficile*. *Appl Environ. Microbiol* **85**, 1–15 (2019).
104. Pyne, M. E., Bruder, M. R., Moo-Young, M., Chung, D. A. & Chou, C. P. Harnessing heterologous and endogenous CRISPR-Cas machineries for efficient markerless genome editing in *Clostridium*. *Sci Rep* **6**, 1–15 (2016).
105. Vento, J. M., Crook, N. & Beisel, C. L. Barriers to genome editing with CRISPR in bacteria. *Journal of Industrial Microbiology and Biotechnology* **46**, 1327–1341 Preprint at https://doi.org/10.1007/s10295-019-02195-1 (2019).
106. Zhang, J., Zong, W., Hong, W., Zhang, Z. T. & Wang, Y. Exploiting endogenous CRISPR-Cas system for multiplex genome editing in clostridium tyrobutyricum and engineer the strain for high-level butanol production. *Metab. Eng.* **47**, 49–59 (2018).
107. Zheng, Y. et al. Characterization and repurposing of the endogenous type I-F CRISPR-Cas system of zymomonas mobilis for genome engineering. *Nucleic Acids Res.* **47**, 11461–11475 (2019).

108. Westra, E. R. et al. CRISPR immunity relies on the consecutive binding and degradation of negatively supercoiled invader DNA by cascade and Cas3. *Mol. Cell.* **46**, 595–605 (2012).
109. Csörgő, B. et al. A compact Cascade–Cas3 system for targeted genome engineering. *Nat. Methods*. **17**, 1183–1190 (2020).
110. Couvin, D. et al. CRISPRCasFinder, an update of CRISRFinder, includes a portable version, enhanced performance and integrates search for Cas proteins. *Nucleic Acids Res.* **46**, W246–W251 (2018).
111. Biswas, A., Gagnon, J. N., Brouns, S. J. J., Fineran, P. C. & Brown, C. M. CRISPRTarget: bioinformatic prediction and analysis of crRNA targets. *RNA Biol.* **10**, 817–827 (2013).
112. Solovyev, V. & Salamov, A. Automatic Annotation of Microbial Genomes and Metagenomic Sequences. In Metagenomics and its Applications in Agriculture, Biomedicine and Environmental Studies (Ed. R.W. Li), Nova Science Publishers, 61–78. (2013).
113. Cassiano, M. H. A. & Silva-Rocha, R. Benchmarking Bacterial Promoter Prediction Tools: Potentialities and Limitations. mSystems, **5**(4), 1–16 e00439-20. https://doi.org/10.1128/mSystems.00439-20 (2020).
114. Sambrook, J. & Russel, D. Molecular Cloning: A Laboratory Manual (Cold Spring Harbor Laboratory Press) - libgen.li, 2001).
115. Choi, K. H. & Schweizer, H. P. mini-Tn7 insertion in bacteria with single attTn7 sites: example *Pseudomonas aeruginosa*. *Nat. Protoc.* **1**, 153–161 (2006).

Acknowledgements

MCM was the recipient of a doctoral scholarship from CONICET. CQ is a member of the CIC from CONICET. This work was supported by grants IP-PUE 0085 from CONICET, ANPCyT 2020-03222 from the Ministry of Science, Technology, and Innovation of Argentina, and PIDAE-UBA 2025 EX-2024-04115022-UBA-DME#REC from the University of Buenos Aires.

Author contributions

C.Q. contributed with conceptualization; designed experiments; performed formal analysis; acquired funding; administered the project; provided resources; supervised; and participated actively in writing the manuscript.M.C.M. contributed with conceptualization; designed and conducted the experiments; performed formal analysis; developed methodology; validated results; prepared presentations for visualization; and took the lead in writing the manuscript.All authors commented on the manuscript.

Declarations

Competing interests

The authors declare no competing interests.

Additional information

Supplementary Information The online version contains supplementary material available at https://doi.org/10.1038/s41598-025-34486-2.

Correspondence and requests for materials should be addressed to C.Q.